ACS APPLIED MATERIALS & INTERFACES

Research Article

www.acsami.org

Biomimetic Choline-Like Graphene Oxide Composites for Neurite Sprouting and Outgrowth

Qin Tu,[†,⊥] Long Pang,[‡,⊥] Lingli Wang,[‡] Yanrong Zhang,[†] Rui Zhang,[§] and Jinyi Wang*[,†,‡]

[†]College of Science and [‡]College of Veterinary Medicine, Northwest A&F University, Yangling, Shaanxi 712100, People's Republic of China

[§]Department of Chemistry & Biochemistry, Florida International University, Miami, Florida 33199, United States

Supporting Information

ABSTRACT: Neurodegenerative diseases or acute injuries of the nervous system always lead to neuron loss and neurite damage. Thus, the development of effective methods to repair these damaged neurons is necessary. The construction of biomimetic materials with specific physicochemical properties is a promising solution to induce neurite sprouting and guide the regenerating nerve. Herein, we present a simple method for constructing biomimetic graphene oxide (GO) composites by covalently bonding an acetylcholine-like unit (dimethylaminoethyl methacrylate, DMAEMA) or phosphorylcholine-like unit (2-methacryloyloxyethyl phosphorylcholine, MPC) onto GO surfaces to enhance neurite sprouting and outgrowth. The resulting GO composites were characterized by Fourier-transform infrared spectroscopy, X-ray photoelectron spectroscopy, Raman spectroscopy, UV−vis spectrometry, scanning electron microscopy, and contact angle analyses. Primary rat hippocampal neurons were used to investigate nerve cell adhesion, spreading, and proliferation on these biomimetic GO composites. GO−DMAEMA and GO−MPC composites provide the desired biomimetic properties for superior biocompatibility without affecting cell viability. At 2 to 7 days after cell seeding was performed, the number of neurites and average neurite length on GO−DMAEMA and GO−MPC composites were significantly enhanced compared with the control GO. In addition, analysis of growth-associate protein-43 (GAP-43) by Western blot showed that GAP-43 expression was greatly improved in biomimetic GO composite groups compared to GO groups, which might promote neurite sprouting and outgrowth. All the results demonstrate the potential of DMAEMA- and MPC-modified GO composites as biomimetic materials for neural interfacing and provide basic information for future biomedical applications of graphene oxide.

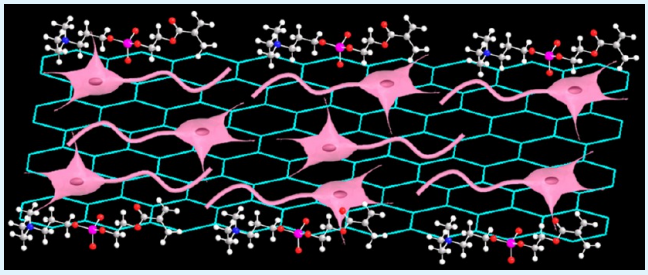

KEYWORDS: *acetylcholine, phosphorylcholine, graphene oxide, neuron, neurite, sprouting, outgrowth*

INTRODUCTION

The nervous system plays an important role in the body; it maintains the body balance by controlling and regulating various body organ activities.[1] Damage to the nervous system can induce the loss of body organ function and further cause some diseases.[2,3] To date, many efforts have been devoted to explore the recovery of the central nervous system after an injury. Generally, promotion of axonal growth[4] and support for long-distance regeneration[5] are the two requirements in the various experimental strategies for nervous system repair.[6] The existing techniques to stimulate and promote axonal growth include grafting of fetal tissue,[7] the peripheral nerve,[8] Schwann cells,[9,10] and olfactory ensheathing cells.[11] Additional options at the molecular level include pharmacological interventions,[12] functional electrical stimulations,[13] and physiotherapies.[14] However, the current state-of-the-art medical treatments have achieved limited success in restoring the functions of severely injured nerves.[15] A promising solution to this challenge is to induce neurite sprouting and guide the regenerating nerve by rationally designed biomaterials.[16−19] Biomimetic materials with proper information content and functionality can direct appropriate cellular activities to sustain and direct cell adhesion, growth, and proliferation and thus to restore or repair damaged or diseased tissues.[17] Recent studies have demonstrated that cellular activities can be influenced by the passive conductivity of a substrate.[20,21] The ability to render biointerfaces electrically conductive opens the possibility of influencing cellular behavior, which can be achieved by utilization of charge conducting polymers[22] and carbon-based materials including carbon nanotubes (CNTs),[20,23] graphite,[24,25] and graphene.[26,27] Among these conductive materials, graphene-based materials have shown novel and superior electrical, chemical, and thermal properties in many research areas.[28,29] The high mobility of charge carriers,[29] intrinsic low electrical noise,[30] and reduced cytotoxicity compared to CNTs[21,31] have made graphene-based materials a very viable candidate for tissue engineering and prosthetics.

Received: September 25, 2013
Accepted: November 29, 2013
Published: November 29, 2013

Scheme 1. Schematic Diagram of the Preparation of GO−DMAEMA and GO−MPC Composites from GO[a]

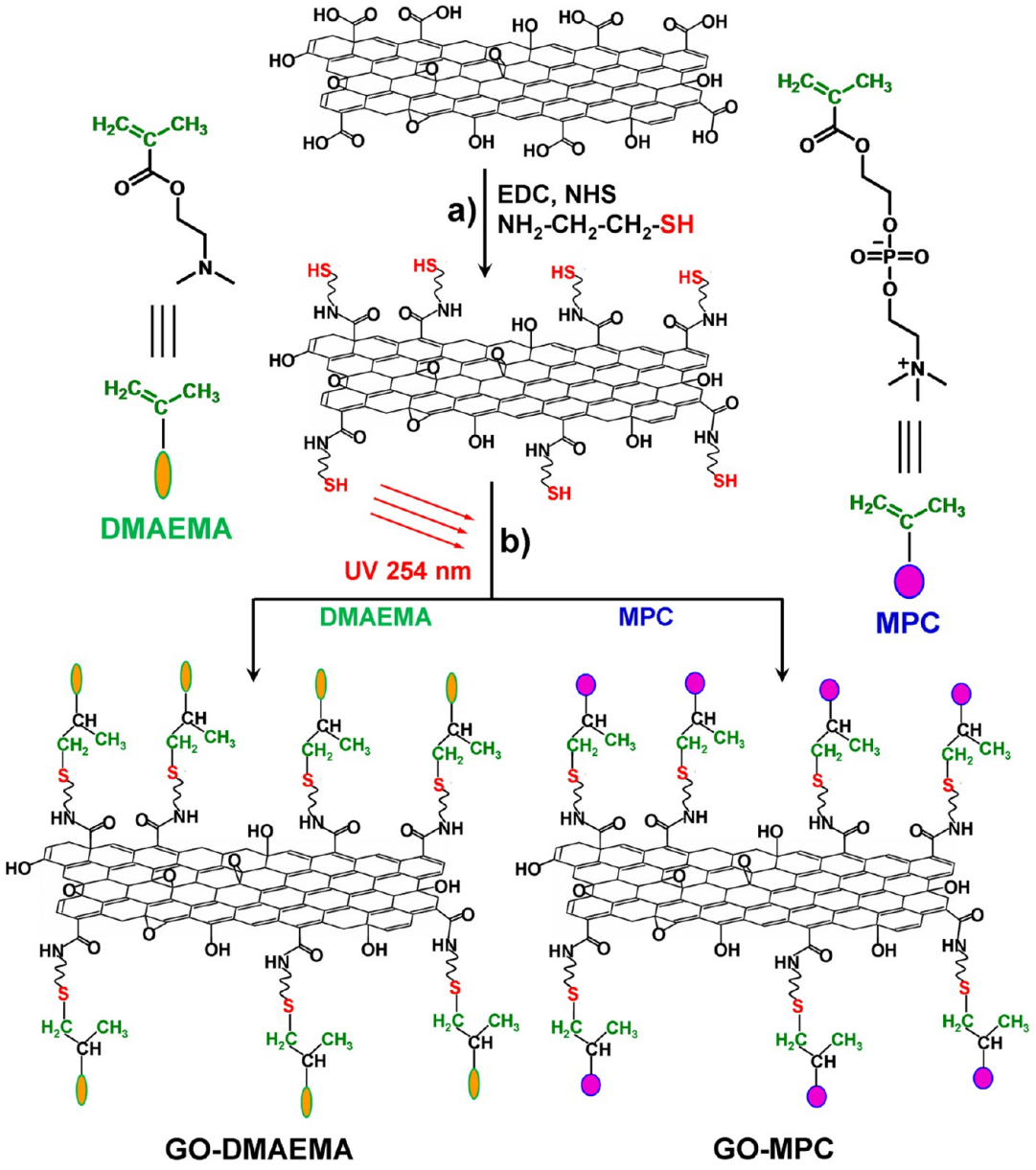

[a]Conditions: (a) EDC/NHS, cysteamine, 48 h; (b) 254 nm UV, DMAEMA/MPC, 24 h.

Graphene, a monolayer of carbon atoms arranged in a 2D honeycomb lattice,[32−34] has inspired great enthusiasm in biomedical fields in recent years owing to its thermal properties, excellent flexibility, electrical conductivity, high strength, stiffness, and biocompatibility.[35] To date, graphene-based materials have already been used in various biomedical fields such as cell imaging, tumor therapy, and so forth.[21,36−39] More recently, the extraordinary properties of graphene-based materials have motivated research groups to use graphene-based material as an ideal biomaterial in tissue engineering and tissue implants.[40] Substrates coated with graphene or graphene oxide have been demonstrated to promote the adhesion and proliferation of several mammalian cells including NIH-3T3 fibroblasts, A549 cells, embryonic cells, and so on.[41−44] According to the properties and biomedical applications of graphene-based materials, the nervous system might be a desired research object.[45−47] Neuronal stimulation and monitoring are necessary for a variety of clinical diagnostics and treatments;[48−50] hence, the unique electrical properties of graphene-based materials offer great advantages for therapeutic or other purposes.[51] Moreover, the chemical stability of graphene-based materials improves the integration with neural tissues. Li et al.[45] recently demonstrated that unmodified graphene possesses good biocompatibility for mouse hippocampal neuron growth. However, an ideal biomaterial should mimic both the structural and biological functions of the native extracellular matrix to provide mechanical support and regulate cellular activities.[52,53] Graphene oxide (GO) contains a range of reactive oxygen functional groups (e.g., −COOH), which render it a good candidate for use in the tissue engineering.[53] However, few reports have described the surface modification of GO with biomimetic functionalities to promote neurite sprouting and outgrowth.

In this study, we explore the construction of smart biomimetic GO composites by covalently bonding an acetylcholine-like unit (dimethylaminoethyl methacrylate, DMAEMA) and a phosphorylcholine-like unit (2-methacryloyloxyethyl phosphorylcholine, MPC) onto GO surfaces to enhance neurite sprouting and outgrowth. Acetylcholine was selected because it is a neurotransmitter and has neuromodulator function in the nervous systems.[54] Phosphorylcholine is part of the platelet-activating factor, a potent and biologically active lipid mediator also present in the nervous tissue[55] where it modulates various cellular functions since it is involved in neuronal differentiation[56] and neurotransmission.[57,58]

EXPERIMENTAL SECTION

Preparation of Thiol-Functionalized Graphene Oxide. The GO solution (1 mg/mL) was ultrasonicated for approximately 8 h before the modification process was performed. The resulting solution was treated with 2.2 mmol/L of 1-ethyl-3-(3-(dimethylamino)propyl) carbodiimide (EDC) and 1.5 mmol/L of *N*-hydroxysuccinimide (NHS) in phosphate-buffered saline (PBS, pH = 7.4). After the carboxyl groups on GO were activated, the solution was treated with 130.6 μmol/L of cysteamine hydrochloride for 1 h and stirred at room temperature for 48 h. The raw product was purified by centrifugation (four times at 14 000 rpm for 4 min each) and washed thrice with ultrapurified water.[59] The thiol-functionalized GO (GO-SH) was finally obtained.

Synthesis of GO−DMAEMA and GO−MPC Composites. The thiol-functionalized GO solution (1 mg/mL, PBS) was ultrasonicated for approximately 8 h. Then, dimethylaminoethyl methacrylate (DMAEMA) or 2-methacryloyloxyethyl phosphorylcholine (MPC) solution (1 mg/mL) was added to the solution to prepare the GO−DMAEMA and GO−MPC composites. The resulting solution was stirred and subjected to 254 nm UV exposure for 24 h. The products were purified by centrifugation and washed thrice using ultrapurified water.[59] GO−DMAEMA and GO−MPC were finally obtained.

Preparation of Graphene Oxide Composite-Coated Glass Coverslips. The solution of each GO composite was prepared by ultrasonication of the GO composite in ethanol (1 mg/mL). Then, 100 μL of each sample solution was spin-coated onto a glass coverslip at 4000 rpm for approximately 30 s. After drying at room temperature, the functional GO film on the slide was obtained.[40] For the blank control slide, GO was used. Glass slides with GO and GO composite films were placed into a culture dish (10 cm in diameter) and treated with UV irradiation for 1 h before use.[54]

Primary Culture of Rat Hippocampal Neuron. The preparation of the primary rat hippocampal neurons used in this work was according to our previous study (for the experimental details, see the Supporting Information).[54] To observe the growth behavior of the primary hippocampal neurons on the biomimetic GO composites, the hippocampal neurons with an initial cell density of 1×10^5 cells/mL were cultured on various GO composite films for one week. Non-neuronal cell division was halted following the methods reported previously.[61,62] Each experiment was repeated at least three times. Control tests were carried out simultaneously.

Cellular Viability. After the samples were cultured on GO composite films for one week, cell viability was assessed according to the acridine orange (AO) and propidium iodide (PI) staining method.[63] After the cultures were rinsed thrice with PBS, then AO (5 mg/mL) and PI (1.0 mmol/L) were added into the neuronal culture dishes. The cultures were incubated at room temperature for 10 min and then rinsed with PBS three times. The cell viability was analyzed by counting the live and dead cells following the method reported previously.[63]

Immunochemistry Staining. The immunochemistry staining assay was performed following the method reported previously.[54] Briefly, the cultured neurons were first fixed with 4% paraformaldehyde at room temperature for 30 min and permeabilized with 0.2% Triton X-100 for another 30 min. The permeabilized neurons were then incubated with 10% newborn calf serum to block nonspecific binding during the immunochemistry assay. After that, the neurons were incubated with mouse anti-MAP2 antibody[64] and rabbit antitau antibody[65] overnight at 4 °C. After washing with PBS, the neurons were further incubated with fluorescence-labeled secondary goat antirabbit antibodies (IgG-FITC; 1:20, primary antibody:PBS, v/v) and goat antimouse (IgG-RBITC; 1:20, primary antibody:PBS, v/v) for 1 h at 37 °C. The neuronal nuclei were stained using Hoechst dye H33258 (0.05 mg/mL).[54]

Image Acquisition and Analysis. All images were obtained using an inverted microscope (Olympus, CKX41). Image and data statistical analyses were performed using software Image-Pro Plus 6.0 (Media Cyternetics) and SPSS 12.0 (SPSS Inc.), respectively. The quantitative data were presented as the mean ± SD. Tests of data significance were performed using one-way ANOVA.

RESULTS AND DISCUSSION

Synthesis and Characterization of GO−DMAEMA and GO−MPC Composites. The preparation (Scheme 1) of the biomimetic GO composites is composed of a two-step reaction. We initially immobilized the thiol-terminated cysteamine onto the GO by activating the carboxyl (−COOH)-rich groups with EDC/NHS chemistry.[59] The bifunctional cysteamine linker carries the amine ($-NH_2$) groups on one side to bind with the carboxyl groups on the GO surface and the thiol (−SH) groups to help anchor the methacrylate-terminated DMAEMA or MPC via the thiol−ene click chemistry under 254 nm UV exposure during the second step.[66,67]

Figure 1 shows the Fourier transform infrared spectroscopy (FT-IR) spectra of the GO, the acetylcholine-like unit modified

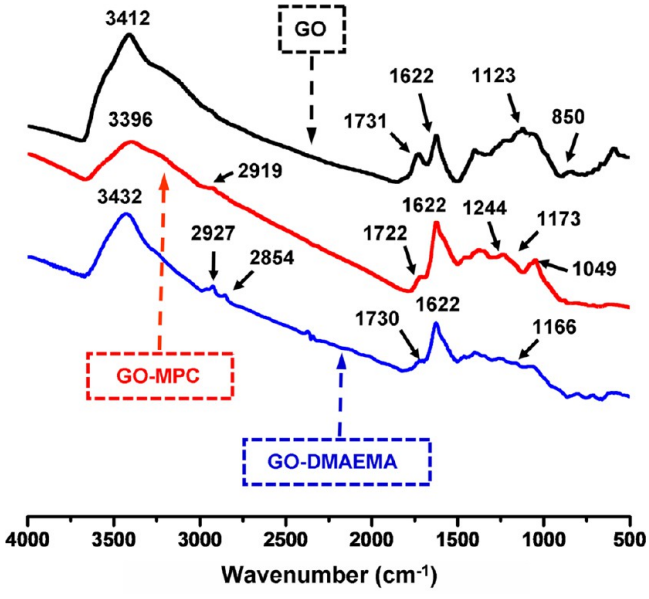

Figure 1. FT-IR spectra of GO (black line), GO−MPC (red line), and GO−DMAEMA (blue line).

GO (GO−DMAEMA), and the phosphorylcholine-like unit modified GO (GO−MPC). The GO spectrum (Figure 1, black line) shows the presence of O−H (ν_{O-H} at 3412 cm^{-1}), C═O ($\nu_{C=O}$ at 1731 cm^{-1} in carbonyl groups), C═C ($\nu_{C=C}$ at 1622 cm^{-1}), and C−O (ν_{C-O} at 1123 and 850 cm^{-1}). In the FT-IR spectrum of GO−SH (Figure S1 in the Supporting Information), peaks at 1557 and 1649 cm^{-1} were assigned to amide (N−H bending) and amide (C═O stretching),

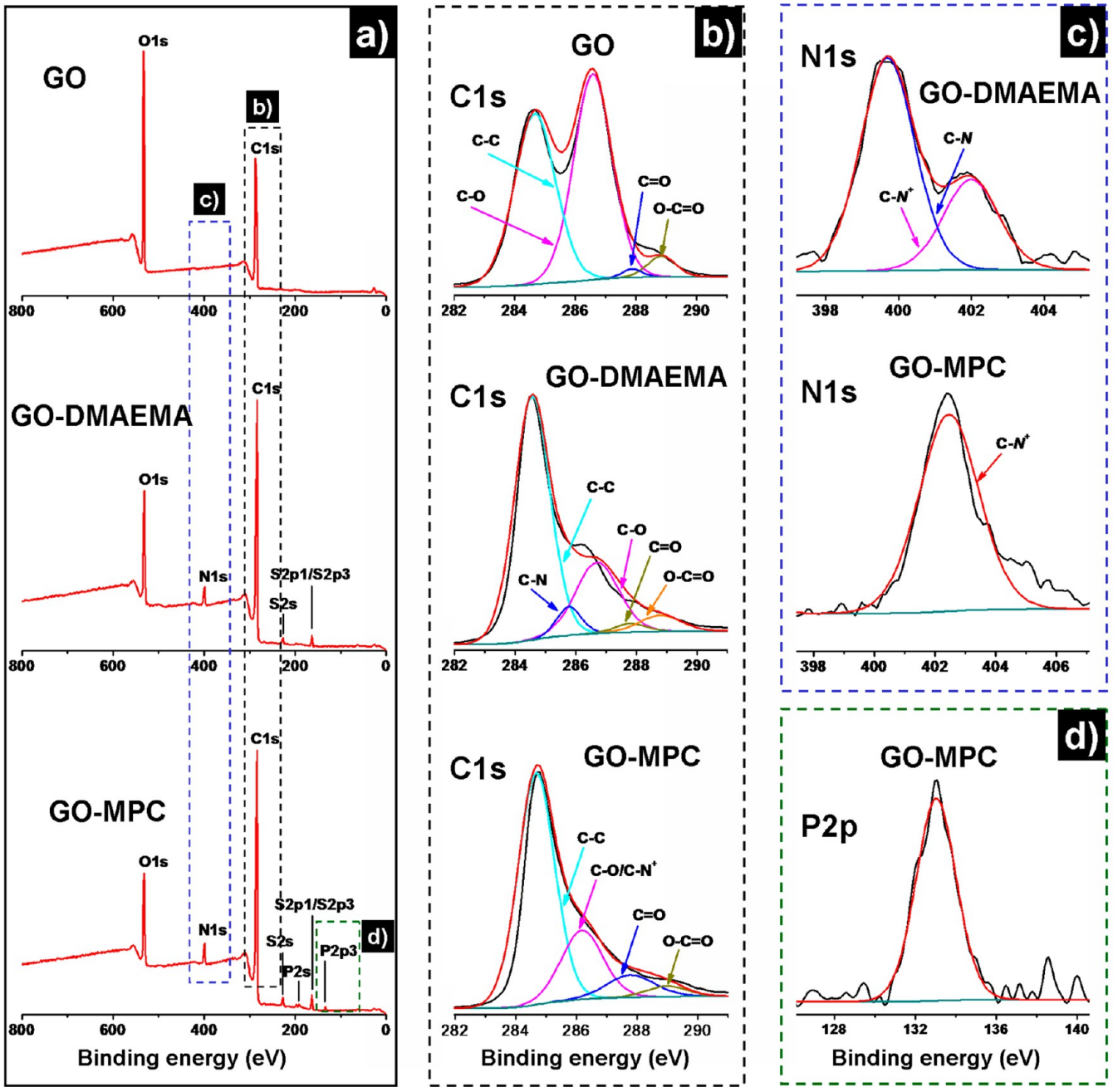

Figure 2. XPS of the GO composites. (a) XPS wide-scan spectra of GO, GO−DMAEMA, and GO−MPC; (b) high-resolution XPS C 1s spectra of GO, GO−DMAEMA, and GO−MPC; (c) high-resolution XPS N 1s spectra of GO−DMAEMA and GO−MPC; and (d) high-resolution XPS P 2p spectrum of GO−MPC.

respectively. The weak absorption peak around 2600 cm^{-1} of S−H stretching vibration was nearly invisible. The peak at 1452 cm^{-1} was assigned to S−CH_2 bending vibration. The typical adsorption peaks of DMAEMA and MPC became visible when the GO was modified with DMAEMA or MPC. The GO−MPC composite spectrum exhibited the characteristic MPC absorption features at 2919 cm^{-1} due to C−H symmetric and asymmetric stretching of methyl and methylene groups, respectively.[50] The peaks (Figure 1, red line) at 1244 and 1049 cm^{-1} were identified as O−P−O antisymmetric stretching in MPC units.[68] In the GO−DMAEMA composite spectrum, the typical absorption peaks of DMAEMA (Figure 1, blue line) at 2927, 2854, and 1166 cm^{-1} correspond to the C−H symmetric and asymmetric stretching of methyl and methylene groups, C−H stretching of the $-N(CH_3)_2$ groups, and C−N stretching of $-N(CH_3)_2$ groups, respectively. The absorption bands at approximately 1730 cm^{-1} in these three spectra correspond to carboxyl groups.[54] These results indicated that DMAEMA and MPC were successfully grafted onto GO.

The formation of GO−MPC and GO−DMAEMA composites was further confirmed by XPS measurements (Figure 2).[40] Only carbon (C 1s at 284.5 eV) and oxygen (O 1s at 532.0 eV) appeared in the wide-scan spectrum of GO (Figure 2a). After GO−DMAEMA and GO−MPC were formed, nitrogen (N 1s at 400.0 eV) and sulfur (S 2s at 227.9 eV) appeared in the wide-scan spectrum. An evident amount of phosphorus (133.9 eV) was present in the GO−MPC in addition to C, O, N, and S (Figure 2a), which were attributed to the phosphorylcholine

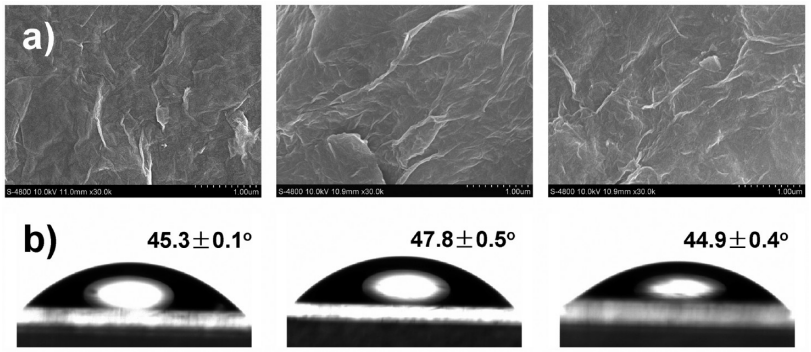

Figure 3. (a) FE-SEM images (30 000× magnification) of GO, GO−DMAEMA, and GO−MPC (from left to right) and (b) the contact angle images of GO, GO−DMAEMA, and GO−MPC (from left to right).

group in the MPC units. XPS analyses revealed that the GO had a small C/O value (1.82). However, the C/O values of GO−DMAEMA and GO−MPC were 4.92 and 5.13, respectively (Table S1 in the Supporting Information), indicating that the introduction of DMAEMA and MPC changed the chemical compositions of the GO surface because more carbon atoms were introduced. Therefore, DMAEMA and MPC were successfully grafted onto the GO sheets.

Further evidence of these composites was obtained through high-resolution XPS spectra (Figures 2b to 2d; the parameters used for fit procedures were summarized in Table S2 in the Supporting Information). The high-resolution C 1s XPS spectra of GO (Figure 2b) exhibited peaks at 284.6 eV (C−C), 286.7 eV (C−O), 287.8 eV (C═O), and 288.7 eV (O−C═O). After DMAEMA was conjugated, the C 1s XPS spectrum of GO−DMAEMA (Figure 2b) showed a significant increase in signals at 284.6 eV, which indicates the increase in C−C functionalities. Moreover, additional absorbance peaks appeared at 285.6 eV, which corresponds to carbon in the C−N bond. These results suggest that GO was functionalized well by DMAEMA. Figure 2c shows the XPS N 1s core-level spectrum of the GO−DMAEMA composite. The N 1s spectrum was resolved into the C−N peak component and the $C-N^+$ peak component with a binding energy of approximately 399.6 and 402.4 eV, respectively.[69] The neutral C−N species of the DMAEMA side chains dominated the total nitrogen species. This information provides supportive evidence that GO was successfully modified with DMAEMA. A significant increase in signals also occurred at 284.6 eV (C−C), and a new peak appeared at 286.7 eV ($C-N^+$) in the C 1s core-level spectrum of the GO−MPC composite (Figure 2b) compared with the C 1s core-level spectrum of GO. The peak at 402.4 eV in the N 1s core-level spectrum of GO−MPC (Figure 2c) corresponds to the nitrogen atom in the MPC quaternary nitrogen, and the P 2p spectrum (Figure 2d) was assigned to P in O−P−O and P═O.[70] These XPS results also suggest that the GO−DMAEMA and GO−MPC nanocomposites were successfully prepared.

Despite being covalently attached to DMAEMA or MPC, the Raman spectra of GO, GO−DMAEMA, and GO−MPC all showed the characteristic tangential mode signals (G band) and disorder mode signals (D band)[71] at 1600 and 1350 cm^{-1}, respectively (Figure S2 in the Supporting Information). In addition, the D/G ratio for GO, GO−DMAEMA, and GO−MPC was nearly constant. The results demonstrated that the functionalized graphene oxide composites still conserved the carbon sp^2 network.[72]

The UV−vis spectra of pure GO, MPC, and DMAEMA in ethanol have absorption peaks at 212, 223, and 225 nm, respectively (Figures S3a−3c in the Supporting Information). After GO−MPC was formed, the absorption peaks of GO−MPC were red-shifted from 212 to 226 nm and 223 to 270 nm because of the interaction between GO sheets and MPC.[54] A similar phenomenon was found in the GO−DMAEMA composite. In particular, the absorption peaks of GO−DMAEMA were red-shifted from 212 to 220 nm and 225 to 270 nm because of the interaction between GO sheets and DMAEMA.[73] These results provided evidence that GO−MPC and GO−DMAEMA composites were obtained. In addition, at concentrations of 0.5 mg/mL, the resulting GO−MPC and GO−DMAEMA solutions were very stable (Figure S3d in the Supporting Information), even for several weeks storage without precipitate, which is very favorable for the further applications of these functionalized GO composites.[73]

The morphologies of the GO, GO−DMAEMA, and GO−MPC composites were studied by field emission (FE)-SEM. The GO, GO−DMAEMA, and GO−MPC (in ethanol) dispersions of 0.5 mg/mL were placed on mica sheets to form a thin layer. The mica sheets were then dried at ambient conditions for 24 h and directly examined under a FE-SEM. The distortions[74] caused by the oxygen groups and the extremely small thickness of the resulting GO sheets led to a wrinkled topology (Figure 3a).

The composite film hydrophilicity was investigated using the sessile drop technique.[54] Figure 3b shows that the contact angles of GO, GO−DMAEMA, and GO−MPC films were 45.3 ± 0.1°, 47.8 ± 0.5°, and 44.9 ± 0.4°, respectively. This result suggests that GO−DMAEMA is slightly more hydrophobic than GO−MPC, which was attributed to the hydrophilicity of the MPC moiety. However, no significant differences were observed in the hydrophilicity of these three materials.

Hippocampal Neuron Attachment to and Proliferation on GO−DMAEMA and GO−MPC Composite Films. To evaluate the effect of the biomimetic GO composites on neuron growth, GO−DMAEMA and GO−MPC composites were separately spin-coated on glass slides.[40] GO was used as the control sample. The GO composite-coated glass slides were then placed into the neuronal culture dishes. The neurons attached and grew on these glass slides. The assays of cellular viability exhibited that the neurons remained alive (green) after being cultured for 7 days on the glass slides that were coated with GO composites (Figure S4 in the Supporting Information). Quantification analysis (Figure S5 in the Supporting Information) of the total number of adherent

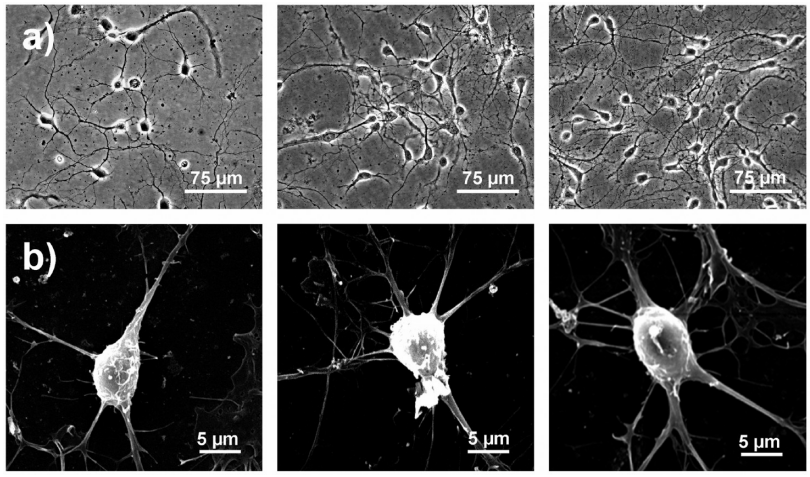

Figure 4. (a) Optical images (400× magnification) of neurons after a 7 day culture on GO, GO−MPC, and GO−DMAEMA films (from left to right) and (b) SEM images (2000× magnification) of neurons after a 7 day culture on GO, GO−MPC, and GO−DMAEMA films (from left to right).

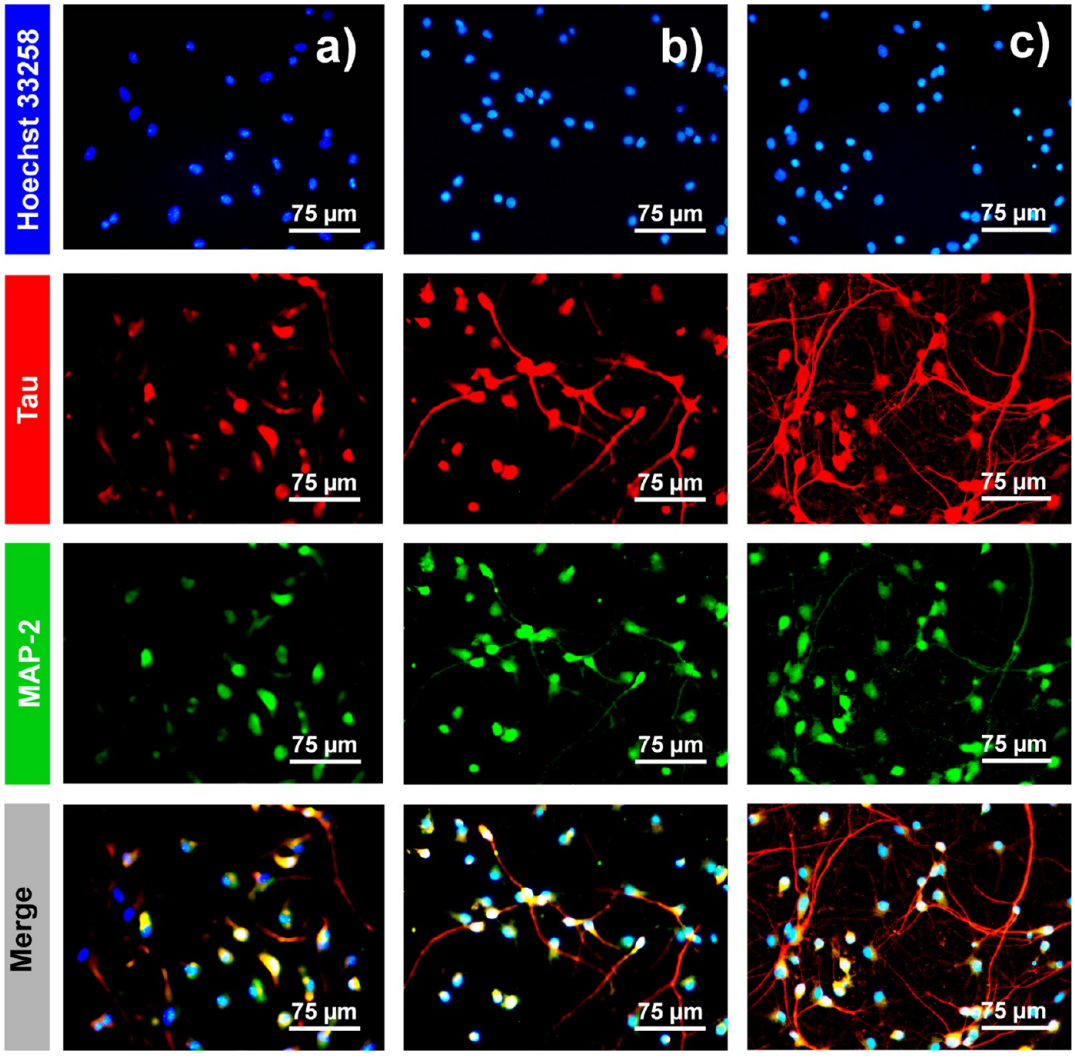

Figure 5. Immunochemistry staining fluorescent hippocampal neuron images (400× magnification) after a 7 day culture on GO (a), GO−MPC (b), and GO−DMAEMA (c) films.

neurons indicated that the viability of neurons can reach over 96% (GO: 97.5%, GO−MPC: 97.1%, and GO−DMAEMA: 96.9%).[45] This result indicates that these GO materials possess good biocompatibility for hippocampal neuron culture.

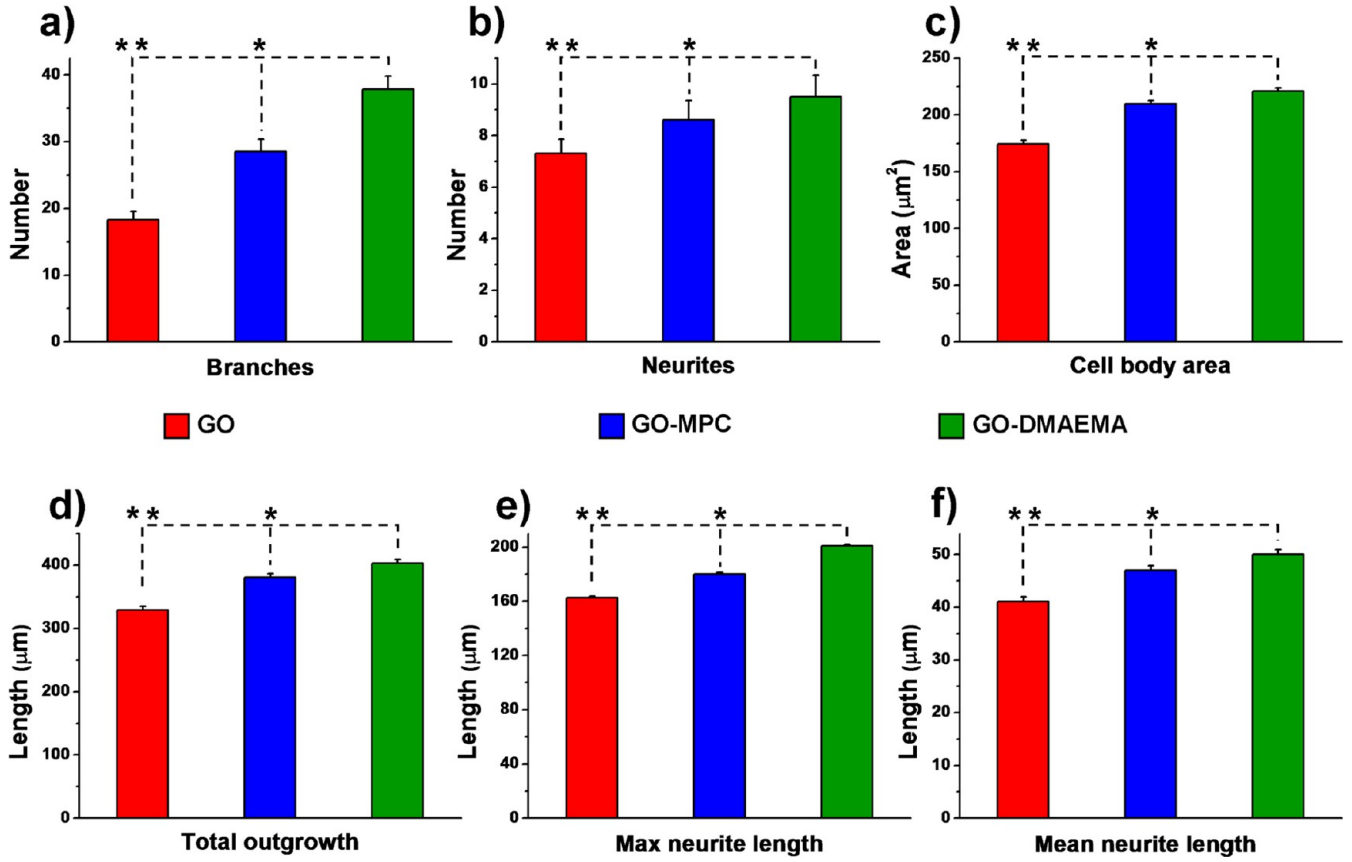

Figure 6. Parameters of hippocampal neuron growth after a 7 day culture on GO, GO−MPC, and GO−DMAEMA films. (a) Branches, (b) neurites, (c) cell body area, (d) total outgrowth, (e) maximum neurite length, and (f) mean neurite length. In this statistical analysis, more than 150 neurons were used for each parameter under the same conditions. Asterisks indicate a significant difference in measurements (one-way ANOVA followed by Fisher's least significant difference test, $*p < 0.05$, $**p < 0.01$).

To further investigate GO composite effects on the growth of hippocampal neurons, cellular shape, particularly neurite change, was used as the main parameter of neuronal growth.[60] Figure 4a shows the representative images of neurons on different films after the samples were incubated for 7 days. These results indicate that hippocampal neurons efficiently attached to and grew on these GO composites. All of the rat hippocampal neurons had a regular cobblestone morphology, apparent neurites, and extensive neurite networks. The SEM image (Figure 4b, for the experimental details, see the Supporting Information) shows that neurite networks were formed by the neurons cultured on biomimetic GO composites after the samples were cultured for 7 days and exhibited normal adhesion and neurite formation. Moreover, a comparison of the neuronal growth on the different films exhibited that the GO−DMAEMA composite film presented the highest number of total outgrowth and branches of each neuron as well as the best networks of neurites, followed by neuron growth on the GO−MPC composite film.

Immunochemistry Staining of the Cultured Hippocampal Neurons on GO−DMAEMA and GO−MPC Films. Immunochemistry staining analysis (Figure 5) showed that most of the culture cells were neurons.[61,62] The micrographs of hippocampal neurons exhibited the marked cell body and longer neurites that spread on the coverslips coated with GO−DMAEMA or GO−MPC composite, compared with those on the control GO-coated coverslips. These findings were similar to those obtained using optical phase-contrast image analysis. Immunochemistry analysis provided supporting evidence that GO−DMAEMA and GO−MPC composites can promote hippocampal neuronal growth. GO−DMAEMA exhibited the most potent ability to promote neuron growth.

Neuronal morphological characteristics were quantified using the neurite application module of software Image-Pro Plus 6.0 (Media Cybernetics, Sliver Spring, MD). The two biomimetic GO composite films we created could, indeed, be used to promote neuron growth. We considered several measurements of neuronal growth to observe the function of DMAEMA- and MPC-modified GO composites (Figure 6). These characteristics likely indicate the possible neuron growth, interconnectivity, and synapse formation. The number of branches and neurites, the area of the cell body, and the length of the total outgrowth as well as maximum and mean neurites of hippocampal neurons were significantly higher in neurons grown on GO−DMAEMA and GO−MPC composite films than those on GO-coated coverslips. Generally speaking, the density, number, and length of neurites were significantly greater in neurons grown on biomimetic GO−DMAEMA and GO−MPC composite films than those on pure GO films. Furthermore, the hippocampal neurons on GO−DMAEMA composite films showed the highest cellular percentage and growth status. Observation of the lamellipodia morphology of neurons and quantitative analysis of the area of the lamellipodia (Figure 7; for the experimental details, see the Supporting Information) showed that the neuron attachment on

biomimetic GO composite films was better than those on the GO film.

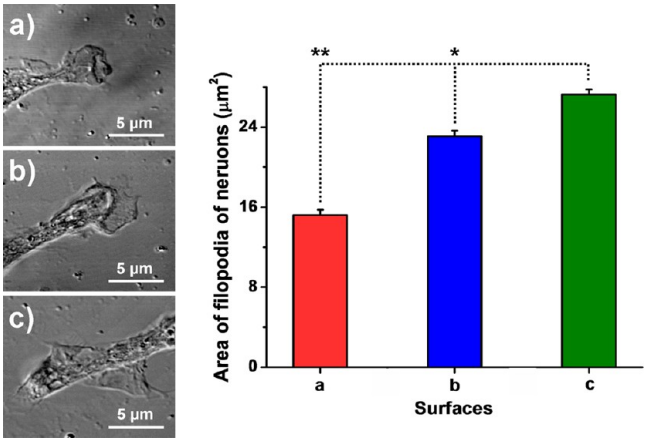

Figure 7. Left column: the optical images of lamellipodia morphology of neurons after a 2 day culture on GO (a), GO−MPC (b), and GO−DMAEMA (c) films. Right column: quantitative analysis of the area of lamellipodia of hippocampal neuron cultured on GO (a), GO−MPC (b), and GO−DMAEMA (c). Asterisks indicate a significant difference in measurements (one-way ANOVA followed by Fisher's least significant difference test, $*p < 0.05$, $**p < 0.01$).

Neurite sprouting and outgrowth is one of the symbols of nervous system development.[75] Therefore, the frequency distribution of neurite lengths was also statistically analyzed from days 2 to 7 (Figure 8). For clarity, the length of the neurite was divided into six sections according to their actual length, i.e., <25, 25−50, 50−75, 75−100, 100−150, and >150 μm. Statistical differences in neurite length between the biomimetic GO composites and the GO were the largest on day 2 compared with those on days 3 to 7, which means that GO−DMAEMA and GO−MPC composites have a strong influence on the early development of neurons. Neurons at this stage are more susceptive to the surrounding environment,[45] which may lead to a more significant impact on day 2 than on other days. Comprehensive analysis of the frequency distribution of neurite lengths also showed that the growth and development of neurites on the biomimetic GO composites (especially the GO−DMAEMA composite) were significantly better than those of neurites grown on the GO; longer neurites appeared more and/or shorter neurites appeared less on the biomimetic GO composites compared with those on the GO.

GAP-43 Expression in Neurons. GAP-43 is a nervous-tissue-specific protein and is expressed at high levels in neuronal growth cones during development.[76] To investigate whether the promotion of neurite outgrowth on biomimetic GO composites was related to GAP-43 upregulation or not, the analysis of GAP-43 expression was performed on day 7 when neurons were mature (for the experimental details, see the Supporting Information).[45] The result (Figure 9a) showed that GAP-43 expression was obviously higher on biomimetic GO composites (especially the GO−DMAEMA composite) than those on GO ($p < 0.05$) (Figure 9b). This suggests that biomimetic GO composites upregulate the expression of GAP-43 protein, which promotes neurite sprouting and outgrowth.[45] However, the further studies on the exact mechanism of the upregulation of GAP-43 expression on biomimetic GO composite films remain necessary.

CONCLUSIONS

In conclusion, the biomimetic choline-like GO composites GO−DMAEMA and GO−MPC were prepared by covalently bonding an acetylcholine-like unit (DMAEMA) and a phosphorylcholine-like unit (MPC) on GO surfaces. The primary rat hippocampal neuron culture demonstrated that these biomimetic choline-like GO composites can significantly boost neurite sprouting and outgrowth compared with pure

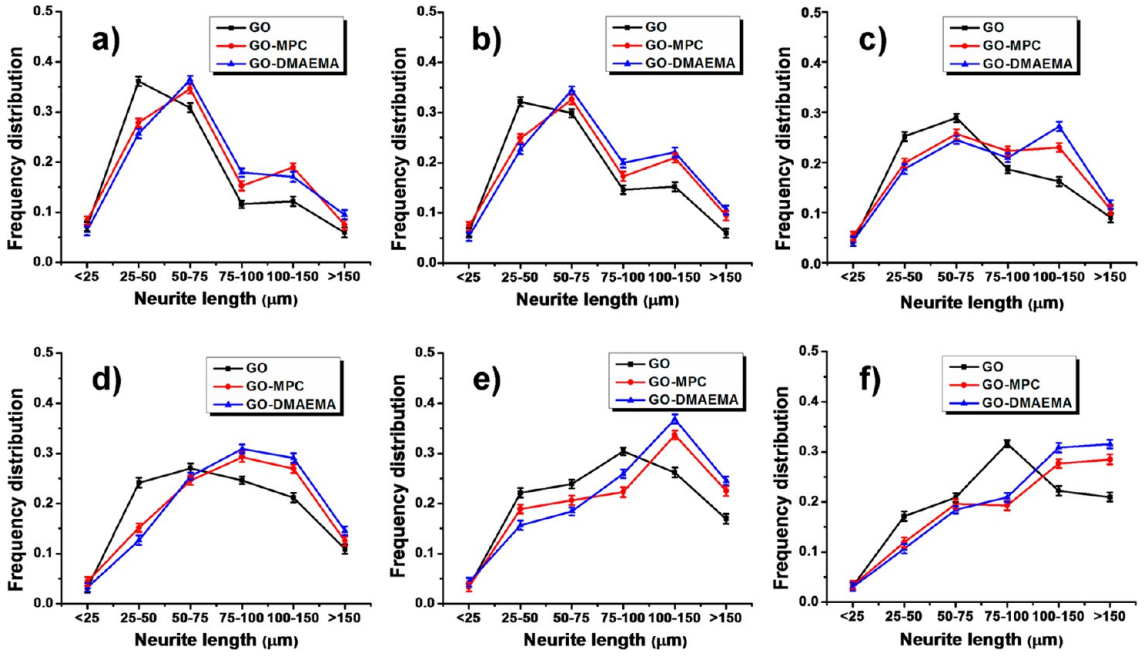

Figure 8. Frequency distribution of the neurite length of neurons cultured on GO, GO−MPC, and GO−DMAEMA films from day 2 to day 7 after they were seeded. (a) Day 2, (b) day 3, (c) day 4, (d) day 5, (e) day 6, and (f) day 7.

dx.doi.org/10.1021/am4042004 | ACS Appl. Mater. Interfaces 2013, 5, 13188−13197

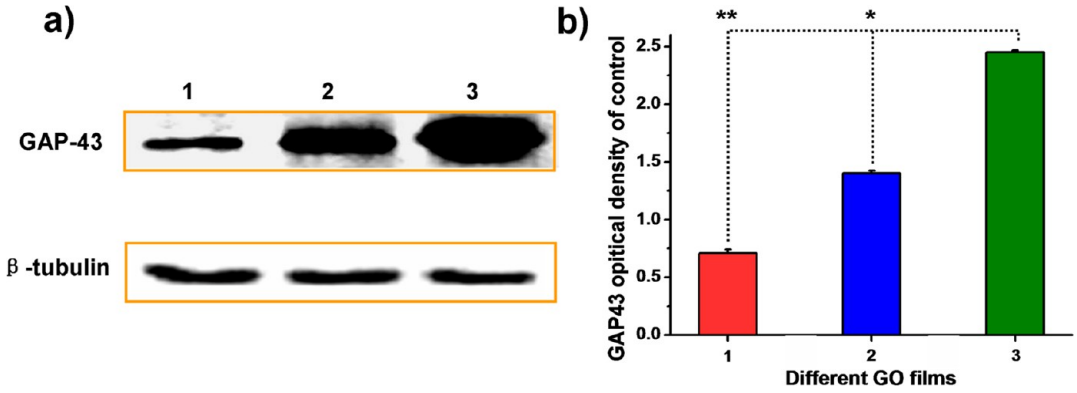

Figure 9. (a) Western blot of GAP-43 expression after neurons were cultured for 7 days on the GO (1), GO−MPC (2), and GO−DMAEMA (3) films. (b) Relative optical densities of GAP-43 bands shown in (a). Asterisks indicate a significant difference in measurements (one-way ANOVA followed by Fisher's least significant difference test, $*p < 0.05$, $**p < 0.01$).

GO. Comparing the two biomimetic composites, GO−DMAEMA was more beneficial to neurite sprouting and outgrowth than GO−MPC. The exact mechanism of the ability of GO−DMAEMA and GO−MPC composites is still under investigation. This study reports an approach that can be used to fabricate GO-based biomimetic materials and provides a better understanding of the biological properties of biomimetic GO−DMAEMA and GO−MPC composites as well as their potential biomedical and biotechnological applications. Due to the interactions of these biomimetic GO composites with neurons, these composites may be potentially used as implanted materials for nerve tissue engineering.

■ ASSOCIATED CONTENT

Supporting Information

Materials and reagents, characterization, primary rat hippocampal neuron culture, SEM observation of neuron morphology, Western blot, FT-IR spectra of GO and GO−SH, elemental composition of different GO composites, the parameters used for fitting C 1s, N 1s, and P 2p peaks, Raman spectra of different GO composites, UV−vis spectroscopy of different GO composites in ethanol, live/dead cell assay, and observation of the lamellipodia morphology of neurons. This material is available free of charge via the Internet at http://pubs.acs.org.

■ AUTHOR INFORMATION

Corresponding Author

*Phone: + 86-29-870 825 20. Fax: + 86-29-870 825 20. E-mail: jywang@nwsuaf.edu.cn.

Author Contributions

⊥Q.T. and L.P. contributed equally to this work.

Notes

The authors declare no competing financial interest.

■ ACKNOWLEDGMENTS

This study was supported by the National Natural Science Foundation of China (21175107 and 21375106) and the Fundamental Research Funds for the Central Universities (Z109021303).

■ REFERENCES

(1) Natalia, O. G.; David, D. G. *Annu. Rev. Neurosci.* **2005**, *28*, 191−222.
(2) Qin, W.; Bauman, W. A.; Cardozo, C. *Ann. N.Y. Acad. Sci.* **2010**, *1211*, 66−84.
(3) Anderson, K. D. *J. Neurotrauma* **2004**, *21*, 1371−1383.
(4) Varga, Z. M.; Fernandez, J.; Blackshaw, S.; Martin, A. R.; Muller, K. J.; Adams, W. B.; Nicholls, J. G. *J. Comp. Neurol.* **1996**, *366*, 600.
(5) Bregman, B. S. *Curr. Opin. Neurobiol.* **1998**, *8*, 800−807.
(6) Tatagiba, M.; Brosamle, C.; Schwab, M. E. *Neurosurgery* **1997**, *40*, 541−547.
(7) Thompson, J. M.; Lu, A. H.; Ruch, S. *Brain Res. Bull.* **1987**, *18*, 479−484.
(8) Sandrock, A. W., Jr.; Matthew, W. D. *Proc. Natl. Acad. Sci. U.S.A.* **1987**, *84*, 6934−6938.
(9) Kleitman, N.; Wood, P.; Johnson, M. I.; Bunge, R. P. *J. Neurosci.* **1988**, *8*, 653−663.
(10) Fallon, J. R. *J. Cell Biol.* **1985**, *100*, 198−207.
(11) Chuah, M. I.; Choi-Lundberg, D.; Weston, S.; Vincent, A. J.; Chung, R. S.; Vickers, J. C.; West, A. K. *Exp. Neurol.* **2004**, *185*, 15−25.
(12) Robinson, D. A.; Zhuo, M. *Methods Mol. Med.* **2003**, *84*, 217−222.
(13) Fujiki, M.; Kobayashi, H.; Isono, M. *Acta Neurochir. Suppl.* **2003**, *86*, 395−397.
(14) Anderson, C. J.; Vogel, L. C. *Spinal Cord* **2003**, *41*, 684−691.
(15) Chalfoun, C. T.; Wirth, G. A.; Evans, G. R. *J. Cell Mol. Med.* **2006**, *10*, 309−317.
(16) Schmidt, C. E.; Leach, J. B. *Annu. Rev. Biomed. Eng.* **2003**, *5*, 293−347.
(17) Gumera, C. B.; Wang, Y. *Adv. Mater.* **2007**, *19*, 4404−4409.
(18) Platt, C. I.; Krekoski, C. A.; Ward, R. V.; Edwards, D. R.; Gavrilovic, J. *J. Neurosci. Res.* **2003**, *74*, 417−429.
(19) Thomas, C. K.; Sesodia, S.; Erb, D. E.; Grumbles, R. M. *Exp. Neurol.* **2003**, *80*, 25−31.
(20) Cellot, G.; Cilia, E.; Cipollone, S.; Rancic, V.; Sucapane, A.; Giordani, S.; Gambazzi, L.; Markram, H.; Grandolfo, M.; Scaini, D.; Gelain, F.; Casalis, L.; Prato, M.; Giugliano, M.; Ballerini, L. *Nat. Nanotechnol.* **2009**, *4*, 126−133.
(21) Park, S. Y.; Park, J.; Sim, S. H.; Sung, M. G.; Kim, K. S.; Hong, B. H.; Hong, S. *Adv. Mater.* **2011**, *23*, H263−H267.
(22) Abidian, M. R.; Ludwig, K. A.; Marzullo, T. C.; Martin, D. C.; Kipke, D. R. *Adv. Mater.* **2009**, *21*, 3764−3770.
(23) Malarkey, E. B.; Fisher, K. A.; Bekyarova, E.; Liu, W.; Haddon, R. C.; Parpura, V. *Nano Lett.* **2008**, *9*, 264−268.
(24) Alazemi, M.; Dutta, I.; Wang, F.; Blunk, R. H.; Angelopoulos, A. P. *Adv. Funct. Mater.* **2009**, *19*, 1118−1129.
(25) Hendricks, T. R.; Lu, J.; Drzal, L. T.; Lee, I. *Adv. Mater.* **2008**, *20*, 2008−2012.
(26) Shen, J.; Hu, Y.; Li, C.; Qin, C.; Shi, M.; Ye, M. *Langmuir* **2009**, *25*, 6122−6128.
(27) Gunes, F.; Shin, H.-J.; Biswas, C.; Han, G. H.; Kim, E. S.; Chae, S. J.; Choi, J.-Y.; Lee, Y. H. *ACS Nano* **2010**, *4*, 4595−4600.

(28) Novoselov, K. S.; Geim, A. K.; Morozov, S. V.; Jiang, D.; Zhang, Y.; Dubonos, S. V.; Grigorieva, I. V.; Firsov, A. A. *Science* **2004**, *306*, 666−669.
(29) Bolotin, K. I.; Sikes, K. J.; Jiang, Z.; Klima, M.; Fudenberg, G.; Hone, J.; Kim, P.; Stormer, H. L. *Solid State Commun.* **2008**, *146*, 351−355.
(30) Zhang, B.; Cui, T. *Appl. Phys. Lett.* **2011**, *98*, 073116.
(31) Zhang, Y.; Ali, S. F.; Dervishi, E.; Xu, Y.; Li, Z.; Casciano, D.; Biris, A. S. *ACS Nano* **2010**, *4*, 3181−3186.
(32) Novoselov, A. *Nat. Mater.* **2007**, *6*, 183−191.
(33) Allen, M. J.; Tung, V. C.; Kaner, R. B. *Chem. Rev.* **2010**, *110*, 132−145.
(34) Meyer, J. C.; Geim, A. K.; Katsnelson, M. I.; Novoselov, K. S.; Booth, T. J.; Roth, S. *Nature* **2007**, *446*, 60−63.
(35) Zhu, Y.; Murali, S.; Cai, W.; Li, X.; Suk, J. W.; Potts, J. R.; Ruoff, R. S. *Adv. Mater.* **2010**, *22*, 3906−3924.
(36) Sun, X.; Liu, Z.; Welsher, K.; Robinson, J. T.; Goodwin, A.; Zaric, S.; Dai, H. *Nano Res.* **2008**, *1*, 203−212.
(37) Cohen-Karni, T.; Qing, Q.; Li, Q.; Fang, Y.; Lieber, C. M. *Nano Lett.* **2010**, *10*, 1098−1102.
(38) Kalbacova, M.; Broz, A.; Kong, J.; Kalbac, M. *Carbon* **2010**, *48*, 4323−4329.
(39) Yang, K.; Zhang, S.; Zhang, G.; Sun, X.; Lee, S.-T.; Liu, Z. *Nano Lett.* **2010**, *10*, 3318−3323.
(40) Some, S.; Ho, S.-M.; Dua, P.; Hwang, E.; Shin, Y. H.; Yoo, H. J.; Kang, J.-S.; Lee, D-ki.; Lee, H. *ACS Nano* **2012**, *6*, 7151−7161.
(41) Ryoo, S. R.; Kim, Y. K.; Kim, M. H.; Min, D. H. *ACS Nano* **2010**, *4*, 6587−6598.
(42) Chen, H.; Muller, M. B.; Gilmore, K. J.; Wallace, G. G.; Li, D. *Adv. Mater.* **2008**, *20*, 3557−3561.
(43) Agarwal, S.; Zhou, X.; Ye, F.; He, Q.; Chen, G. C.; Soo, J.; Boey, F.; Zhang, H.; Chen, P. *Langmuir* **2010**, *26*, 2244−2247.
(44) Park, S.; Mohanty, N.; Suk, J. W.; Nagaraja, A.; An, J.; Piner, R. D.; Cai, W.; Dreyer, D. B.; Berry, V.; Ruoff, R. S. *Adv. Mater.* **2010**, *22*, 1736−1740.
(45) Li, N.; Zhang, X.; Song, Q.; Su, R.; Zhang, Q.; Kong, T.; Liu, L.; Jin, G.; Tang, M.; Cheng, G. *Biomaterials* **2011**, *32*, 9374−9382.
(46) Kim, S. -M.; Joo, P.; Ahn, G.; Cho, I. H.; Kim, D. H.; Song, W. K.; Kim, B. -S.; Yoon, M. -H. *J. Biomed. Nanotechnol.* **2013**, *9*, 403−408.
(47) Lorenzoni, M.; Brandi, F.; Dante, S.; Giugni, A.; Torre, B. *Sci. Rep* **2013**, 3.
(48) Wilson, B. S.; Lawson, D. T.; Muller, J. M.; Tyler, R. S.; Kiefer, J. *Annu. Rev. Biomed. Eng.* **2003**, *5*, 207−249.
(49) Weiland, J. D.; Liu, W. T.; Humayun, M. S. *Annu. Rev. Biomed. Eng.* **2005**, *7*, 361−401.
(50) Navarro, X.; Krueger, T. B.; Lago, N.; Micera, S.; Stieglitz, T.; Dario, P. A. *J. Peripher. Nerv. Syst.* **2005**, *10*, 229−258.
(51) Kotov, N. A.; Winter, J. O.; Clements, I. P.; Jan, E.; Timko, B. P.; Campidelli, S.; Pathak, S.; Mazzatenta, A.; Lieber, C. M.; Prato, M.; Bellamkonda, R. V.; Silva, G. A.; Kam, N. W. S.; Patolsky, F.; Ballerini, L. *Adv. Mater.* **2009**, *21*, 3970−4004.
(52) Park, K. E.; Kang, H. K.; Lee, S. J.; Min, B.-M.; Park, W. H. *Biomacromolecules* **2006**, *7*, 635−643.
(53) Dreyer, D. R.; Park, S.; Bielawski, C. W.; Ruoff, R. S. *Chem. Soc. Rev.* **2010**, *39*, 228−240.
(54) Tu, Q.; Li, L.; Zhang, Y. R.; Wang, J. C.; Liu, R.; Li, M. L.; Liu, W. M.; Wang, X. Q.; Ren, L.; Wang, J. Y. *Biomaterials* **2011**, *32*, 3253−3264.
(55) Tokumura, A.; Kamiyasu, K.; Takanchi, K.; Tsukatani, H. *Biochem. Biophys. Res. Commun.* **1987**, *145*, 415−425.
(56) Kornecki, E.; Ehrlich, Y. H. *Science* **1988**, *240*, 1792−1794.
(57) Bussolino, F.; Gremo, F.; Tetta, C.; Pescarmona, G. P.; Camussi, G. *J. Biol. Chem.* **1986**, *261*, 16502−16508.
(58) Bussolino, F.; Pescarmona, G.; Camussi, G.; Gremo, F. *J. Neurochem.* **1988**, *51*, 1755−1759.
(59) Gulbakan, B.; Yasun, E.; Ibrahim Shukoor, M.; Zhu, Z.; You, M.; Tan, X.; Sanchez, H.; Powell, D. H.; Dai, H.; Tan, W. *J. Am. Chem. Soc.* **2010**, *132*, 17408−17410.
(60) Ivins, K. J.; Bui, E. T.; Cotman, C. W. *Neurobiol. Dis.* **1998**, *5*, 365−378.
(61) Nicole, O.; Ali, C. F.; Docagne, L.; Plawinski, E. T.; MacKenzie, D. V.; Buisson, A. *J. Neurosci.* **2001**, *21*, 3024−3033.
(62) Nault, F.; Koninck, P. D. Dissociated Hippocampal Cultures. In *Protocls for Neural Cell Culture*, 4th ed.; Doering, L. C., Ed.; McMaster University: Canada, 2010; pp 137−159.
(63) Dietz, G. P. H.; Dietz, B.; Bähr, M. *Brain Res.* **2007**, *1164*, 136−141.
(64) Buddle, M.; Eberhardt, E.; Ciminello, L. H.; Levin, T.; Wing, R.; DiPasqualea, K.; Raley-Susman, K. M. *Brain Res.* **2003**, *978*, 38−50.
(65) Mailliot, C.; Bussière, T.; Caillet-Boudin, M.; Delacourte, A.; Buée, L. *Neurosci. Lett.* **1998**, *255*, 13−16.
(66) Rossow, T.; Heyman, J. A.; Ehrlicher, A. J.; Langhoff, A.; Weitz, D. A.; Haag, R.; Seiffert, S. *J. Am. Chem. Soc.* **2012**, *134*, 4983−4989.
(67) Yang, L. Y.; Li, L.; Tu, Q.; Ren, L.; Zhang, Y. R.; Wang, X. Q.; Zhang, Z.; Liu, W.; Xin, L.; Wang, J. *Anal. Chem.* **2010**, *82*, 6430−6439.
(68) Bi, H. Y.; Zhong, W.; Meng, S.; Kong, J. L.; Yang, P. Y.; Liu, B. H. *Anal. Chem.* **2006**, *78*, 3399−3405.
(69) Zhai, G.; Shi, Z. L.; Kang, E. T.; Neoh, K. G. *Macromol. Biosci.* **2005**, *5*, 974−982.
(70) Xu, Y.; Takai, M.; Ishihara, K. *Biomaterials* **2009**, *30*, 4930−4938.
(71) Kudin, K. N.; Ozbas, B.; Schniepp, H. C.; Prud'homme, R. K.; Aksay, I. A.; Car, R. *Nano Lett.* **2008**, *8*, 36−41.
(72) Fang, M.; Wang, K.; Lu, H.; Yang, Y.; Nutt, S. *J. Mater. Chem.* **2009**, *19*, 7098−7105.
(73) Shan, C.; Yang, H.; Han, D.; Zhang, Q.; Ivaska, A.; Niu, L. *Langmuir* **2009**, *25*, 12030−12033.
(74) Yang, H.; Li, F.; Shan, C.; Han, D.; Zhang, Q.; Niu, L.; Ivaska, A. *J. Mater. Chem.* **2009**, *19*, 4632−4638.
(75) Rogers, S. L.; Letourneau, P. C.; Palm, S. L.; McCarthy, J.; Furcht, L. T. *Dev. Biol.* **1983**, *98*, 212−220.
(76) Meiri, K. F.; Pfenninger, K. H.; Willard, M. B. *Proc. Natl. Acad. Sci. U.S.A.* **1986**, *83*, 3537−3541.